MRG15 is required for pre-mRNA splicing and spermatogenesis

Naoki Iwamori[a,b,c,d,1], Kaoru Tominaga[e], Tetsuya Sato[f], Kevin Riehle[g,h], Tokuko Iwamori[a,b,c], Yasuyuki Ohkawa[i], Cristian Coarfa[h,j], Etsuro Ono[a,b], and Martin M. Matzuk[c,d,g,j,k,l,1]

[a]Laboratory of Biomedicine, Division of Pathobiology, Department of Basic Medicine, Faculty of Medicine, Kyushu University, Fukuoka 812-8582, Japan; [b]Center of Biomedical Research, Research Center for Human Disease Modeling, Graduate School of Medical Sciences, Kyushu University, Fukuoka 812-8582, Japan; [c]Department of Pathology and Immunology, Baylor College of Medicine, Houston, TX 77030; [d]Center for Reproductive Medicine, Baylor College of Medicine, Houston, TX 77030; [e]Division of Functional Biochemistry, Department of Biochemistry, Jichi Medical University, Tochigi 329-0498, Japan; [f]Division of Bioinformatics, Medical Institute of Bioregulation, Kyushu University, Fukuoka 812-8582, Japan; [g]Department of Molecular and Human Genetics, Baylor College of Medicine, Houston, TX 77030; [h]Bioinformatics Research Laboratory, Baylor College of Medicine, Houston, TX 77030; [i]Division of Transcriptomics, Medical Institute of Bioregulation, Kyushu University, Fukuoka 812-8582, Japan; [j]Department of Molecular and Cellular Biology, Baylor College of Medicine, Houston, TX 77030; [k]Department of Pharmacology, Baylor College of Medicine, Houston, TX 77030; and [l]Center for Drug Discovery, Baylor College of Medicine, Houston, TX 77030

Contributed by Martin M. Matzuk, July 25, 2016 (sent for review April 1, 2016; reviewed by Alex Bortvin and Robert E. Braun)

Splicing can be epigenetically regulated and involved in cellular differentiation in somatic cells, but the interplay of epigenetic factors and the splicing machinery during spermatogenesis remains unclear. To study these interactions in vivo, we generated a germline deletion of MORF-related gene on chromosome 15 (MRG15), a multifunctional chromatin organizer that binds to methylated histone H3 lysine 36 (H3K36) in introns of transcriptionally active genes and has been implicated in regulation of histone acetylation, homology-directed DNA repair, and alternative splicing in somatic cells. Conditional KO (cKO) males lacking MRG15 in the germline are sterile secondary to spermatogenic arrest at the round spermatid stage. There were no significant alterations in meiotic division and histone acetylation. Specific mRNA sequences disappeared from 66 germ cell-expressed genes in the absence of MRG15, and specific intronic sequences were retained in mRNAs of 4 genes in the MRG15 cKO testes. In particular, introns were retained in mRNAs encoding the transition proteins that replace histones during sperm chromatin condensation. In round spermatids, MRG15 colocalizes with splicing factors PTBP1 and PTBP2 at H3K36me3 sites between the exons and single intron of transition nuclear protein 2 (*Tnp2*). Thus, our results reveal that MRG15 is essential for pre-mRNA splicing during spermatogenesis and that epigenetic regulation of pre-mRNA splicing by histone modification could be useful to understand not only spermatogenesis but also, epigenetic disorders underlying male infertile patients.

infertility | fertility defects | splicing defects | epigenetics | spermiogenesis

Spermatogenesis is a complex process involving several biological events and dramatic changes of chromatin structure. Male germ cells undergo stem cell self-renewal, mitotic divisions in spermatogonial proliferation, genomic rearrangement by meiotic homologous recombination at the spermatocyte stage, and morphological changes of round spermatids into elongated spermatids to form mature spermatozoa (1–3). During spermiogenesis, nucleosomal histone proteins are replaced with transition nuclear proteins (TNPs) and subsequently, protamines, the major nucleosomal proteins in spermatozoa. Moreover, epigenetic modifications, such as histone methylation, dramatically change throughout spermatogenesis (3, 4).

Pre-mRNA splicing generates protein diversity and is involved in the regulation of cellular differentiation (5, 6). Recent advances have shown that histone modifications regulate alternative splicing through recruitment of splicing regulators via chromatin binding proteins, such as MORF-related gene on chromosome 15 (MRG15) (7). Histone H3 lysine 36 (H3K36) is methylated proximal to tissue-specific splicing regions (8–12). MRG15 specifically recognizes the methylated H3K36 and recruits polypyrimidine tract binding protein (PTB) at intronic splicing silencer elements near an exon to suppress exon insertions into mRNA (7). MRG15 is also a component of histone acetyltransferase (HAT) and histone deacetylase (HDAC) complexes and regulates transcription by balancing histone acetylation (7, 13–21). During spermatogenesis, before histones are replaced with transition proteins and protamines, histone H4 is highly acetylated, and the acetylation of histones is required for histone removal. In addition to regulation of pre-mRNA splicing and histone acetylation, MRG15 contributes to homology-directed DNA repair. Although MRG15 functions in multiple biological processes, the roles of MRG15 during spermatogenesis are unknown, because *Mrg15* null mice are embryonic lethal (22).

In this report, we have deleted MRG15 specifically in postnatal male germ cells and analyzed the role of MRG15 during spermatogenesis. Spermatogenesis in the *Mrg15* null testis arrests at the round spermatid stage without affecting meiotic division and histone acetylation. MRG15 contributes to epigenetic regulation of pre-mRNA splicing of *Tnp2*, one of the reasons for the arrest of spermatogenesis in the *Mrg15* null germ cells.

Results

MRG15 Is Required for Postmeiotic Spermatogenesis. MRG15 mRNA levels are extremely high in testis, and expression initiates at 20 d after birth, when late-stage spermatocytes differentiate into round

Significance

Pre-mRNA splicing generates protein diversity, is involved in the regulation of cellular differentiation, and can be epigenetically regulated by histone modifications. Chromatin binding proteins, which recognize histone modifications, recruit splicing regulators to methylated histones around tissue-specific splicing regions and regulate pre-mRNA splicing. However, the interplay of epigenetic factors and the splicing machinery during spermatogenesis remains unclear. Here, we show that epigenetic regulation of pre-mRNA splicing is required for spermatogenesis and male fertility. Thus, novel splicing diversity is important for spermatogenesis, and defects in this system may trigger disease.

Author contributions: N.I., K.T., and M.M.M. designed research; N.I., T.I., and E.O. performed research; N.I. and K.T. contributed new reagents/analytic tools; N.I., T.S., K.R., Y.O., C.C., and M.M.M. analyzed data; and N.I. and M.M.M. wrote the paper.

Reviewers: A.B., Carnegie Institution of Washington; and R.E.B., The Jackson Laboratory.

The authors declare no conflict of interest.

Data deposition: The RNA sequencing and ChIP sequencing data have been deposited in the DDBJ Sequence Read Archive (DRA; accession nos. DRA004783 and DRA004778, respectively).

[1]To whom correspondence may be addressed. Email: iwamori@anim.med.kyushu-u.ac.jp or mmatzuk@bcm.edu.

This article contains supporting information online at www.pnas.org/lookup/suppl/doi:10.1073/pnas.1611995113/-/DCSupplemental.

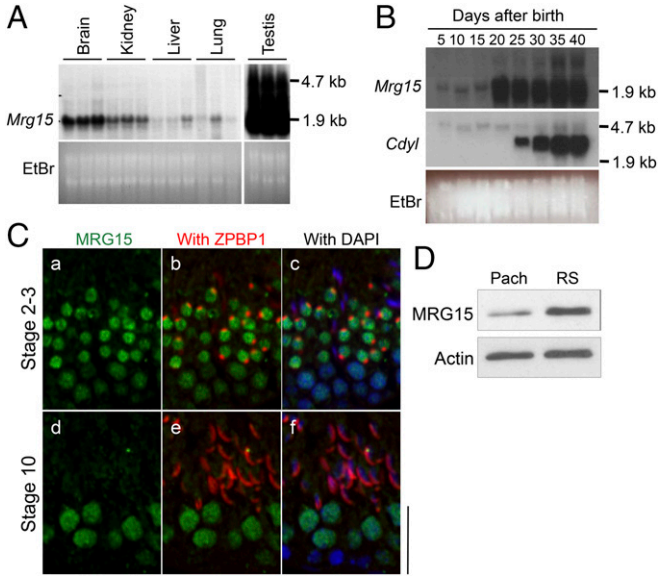

Fig. 1. Spatiotemporal expression of MRG15 in the testis. (*A* and *B*) Transcripts of *Mrg15* were examined by Northern blot analysis (*A*) in multiple tissues and (*B*) during postnatal development of the testis. Expression of chromodomain protein, Y chromosome-like (*Cdyl*) and/or ethidium bromide (EtBr) staining were performed as controls. The testis lanes in *A* were separately exposed to avoid strong radioactive signal from the testis lanes from invading adjacent lanes. (*C*) Immunolocalization of MRG15 in the testes. MRG15 (green), ZPBP1 (red), and DAPI (blue) localization in (*a*–*c*) stages 2 and 3 and (*d*–*f*) stage 10 seminiferous epithelium is shown. Seminiferous stages were determined by patterns of an acrosome staining of ZPBP1. (Scale bar: 10 μm.) (*D*) Western blot analysis of MRG15 in purified pachytene spermatocytes (Pach) and round spermatids (RS). Expression analysis of actin was performed as a control.

spermatids (Fig. 1 *A* and *B*). MRG15 protein localizes in spermatocytes, and its expression is highest in round spermatids during spermatogenesis (Fig. 1 *C* and *D*). To address the in vivo postnatal roles of MRG15 during spermatogenesis, an MRG15-floxed allele was generated in ES cells, and mice carrying this allele were crossed with *Stra8-Cre* mice to achieve germline-specific deletion (*SI Appendix*, Fig. S1) (23). Germline-specific *Mrg15* null males have smaller testes and are sterile compared with control males (Fig. 2 *A*–*C*). In the *Mrg15* null testes, spermatogenesis is arrested at the round spermatid stage, abnormal multinucleated cells are abundant, and there are no detectable mature sperm with condensed nuclei (Fig. 2*D*). Whereas spermatogonia and spermatocytes are histologically normal in *Mrg15* null testes, spermatogenesis is arrested before round spermatid step 7, with significant apoptotic cell death (Fig. 2*E* and *SI Appendix*, Fig. S2). These findings suggest that MRG15 functions in round spermatids or late-stage spermatocytes for progression of spermatogenesis.

MRG15 Is Not Required for Meiotic Progression. Because MRG15 plays an essential role during homology-directed DNA damage repair, SCP1, γH2AX, and ubiquitylated H2A were analyzed in spermatocytes to examine whether MRG15 is required for meiotic homologous recombination (20, 21, 24). However, there were no significant differences in localizations of meiosis regulating proteins between control and *Mrg15* null testes (*SI Appendix*, Figs. S3 and S4*A*). H3K36me3 and H4K20me3, both of which are recognized by MRG15, were not changed by lack of MRG15, indicating that MRG15 is not essential for meiotic homologous recombination (*SI Appendix*, Fig. S3) (25, 26).

Spermatogenesis in *Mrg15* Null Testes Arrests Before Hyperacetylation of Histone H4. During spermatogenesis, histone H4 is highly acetylated before replacement of nucleosomal proteins from histones to TNPs to protamines (27). Because MRG15 is found in both HAT and HDAC complexes (13–21), MRG15 may be essential for postmeiotic events. To investigate whether MRG15 is involved in histone acetylation in postmeiotic spermatogenesis, acetylated histones were analyzed. Although acetylated histone H3 is highly localized in elongated spermatids in control testes, acetylated histone H3 levels in round spermatids are not significantly different between control and MRG15 conditional KO (cKO) testes (*SI Appendix*, Fig. S4*B*). CDYL, a histone H4 acetyltransferase that recognizes methylated H3K9 and is expressed in the testes after postnatal day 25 (Fig. 1*B*), is detectable in elongating spermatids in control testes but not in MRG15 cKO testes, probably because spermatogenesis is arrested before the elongating spermatid stage (*SI Appendix*, Fig. S4*C*) (28). When acetylation of lysines 5, 8, 12, and 16 of histone H4 was analyzed, these acetylated forms were reduced in the *Mrg15* null testes (Fig. 3 and *SI Appendix*, Fig. S5). However, high accumulation of acetylation on each residue was observed in elongating spermatids of control testes, and these germ cells are no longer present in *Mrg15* null testes (Fig. 3 and *SI Appendix*, Fig. S5*A*). When the amounts of histone H4 acetylation on each residue were compared in spermatid fractions between 22-d-old WT testes, in which spermatogenesis has developed to the round spermatid stage, and adult *Mrg15* null testes, there were no significant differences (*SI Appendix*, Fig. S5*B*). Because

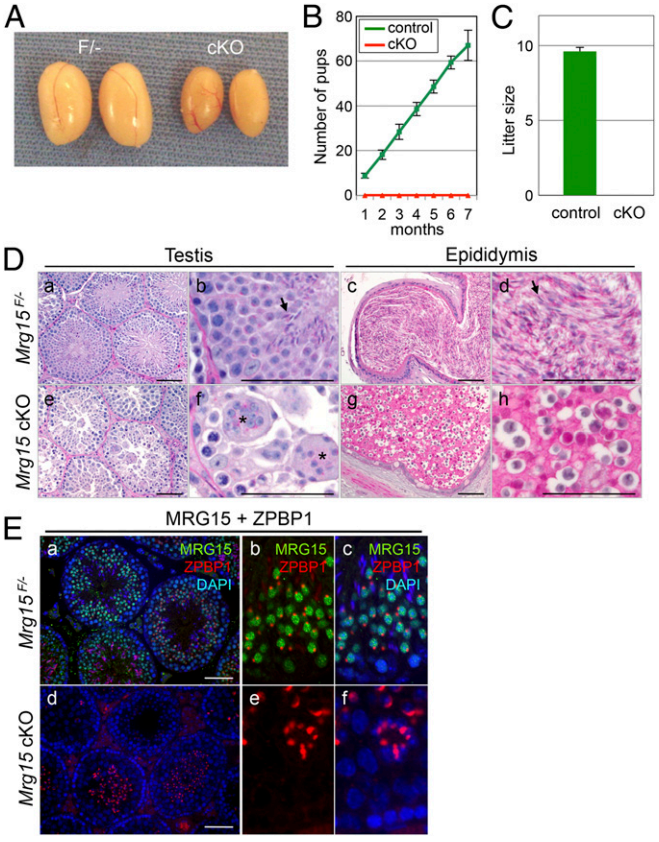

Fig. 2. Infertile phenotype of germ cell-specific MRG15 null mice. (*A*) Gross images of $Mrg15^{F-}$ (F/–) and $Mrg15^{F/-;Stra8\text{-}Cre+}$ (cKO) testes at 10 wk of age. (*B*) Average number of pups produced by F/– (control) and cKO males over 6 mo of breeding ($n = 10$ per genotype). (*C*) Average litter size produced by control and cKO males. (*D*) Histological analyses of (*a*, *b*, *e*, and *f*) testes and (*c*, *d*, *g*, and *h*) epididymis of (*a*–*d*) control and (*e*–*h*) cKO at 10 wk of age. Arrows and asterisks indicate mature sperm and abnormal multinucleated cells, respectively. (Scale bar: 50 μm.) (*E*) Validation of seminiferous stage of spermatogenetic arrest by lack of MRG15. MRG15 (green), ZPBP1 (red), and DAPI (blue) in (*a*–*c*) control and (*d*–*f*) cKO are shown. (Scale bar: 50 μm.)

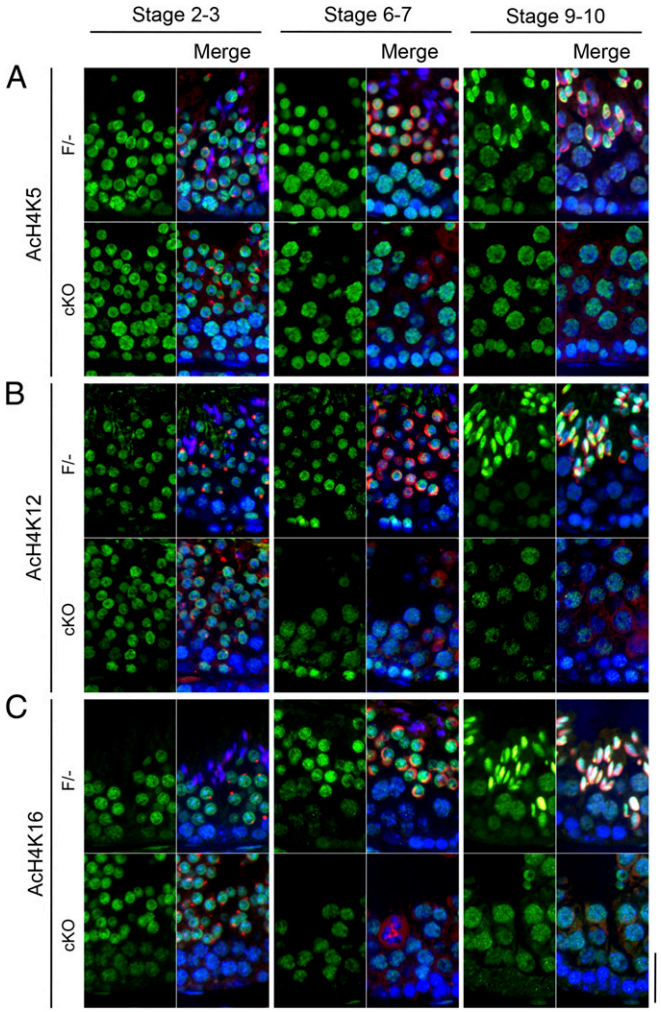

Fig. 3. Analyses of histone acetylation in MRG15 null spermatogenesis. Immunolocalization of acetylated histones in seminiferous cycle. Immunolocalization of (*A*) AcH4K5, (*B*) AcH4K12, and (*C*) AcH4K16 in stages 2 and 3, 6 and 7, and 9 and 10 of seminiferous cycles of both F/– and cKO are shown. Blue, DAPI; green, acetylated histones; red, ZPBP1. (Scale bar: 50 μm.)

spermatogenesis in *Mrg15* null testes arrests at the round spermatid stage before histone H4 is hyperacetylated, it is difficult to determine if MRG15 is necessary for replacement of nucleosomal proteins.

Histone Modification Regulates Splicing of *Tnp2* by MRG15. To study these processes in more molecular detail, expression of protamines (*Prm1* and *Prm2*) and Tnps (*Tnp1* and *Tnp2*) in testes and spermatids was analyzed in WT and *Mrg15* null spermatid fraction. Expression levels of both *Prm* and *Tnp* genes were significantly reduced in the *Mrg15* null adult testes, possibly because the expression of these proteins is the highest in latter stages of spermiogenesis, which are absent in the *Mrg15* null testes (Fig. 4*A*). To further interpret our data, expression of the *Prm* and *Tnp* genes was compared between spermatids fractions isolated from 22-d-old WT and *Mrg15* null testes, in which spermatogenesis has progressed to the early stage of round spermatids. Whereas expression levels of *Prm1* and *Prm2* are decreased in the absence of MRG15, *Tnp1* and *Tnp2* expression levels are not changed by *Mrg15* deletion (Fig. 4*B*). However, the *Tnp2* PCR products were larger in size in the absence of MRG15, and the shifts in size of the larger bands were exactly the size of the *Tnp2* intron sequences (Fig. 4*C*). Larger bands in the absence of MRG15 were also detected in the *Prm2* amplification in the spermatid-enriched fraction, although the larger bands were not observed in 4-wk-old testes. When expression of TNP2 protein was analyzed in the spermatid fraction, the amount of TNP2 (16 kDa) was extremely low in the absence of MRG15 compared with control testis, and a larger TNP2 protein was detected specifically in *Mrg15* null spermatids (Fig. 4*D*), suggesting that splicing of the *Tnp2* gene (Fig. 4*E*) could be regulated by MRG15.

Because MRG15 regulates alternative splicing with recognition of methylated H3K36 and cooperation of PTB proteins, localization of methylated H3K36 and interaction between MRG15 and PTB proteins were analyzed. Methylated H3K36 is detected in a variety of male germ cells and observed at high

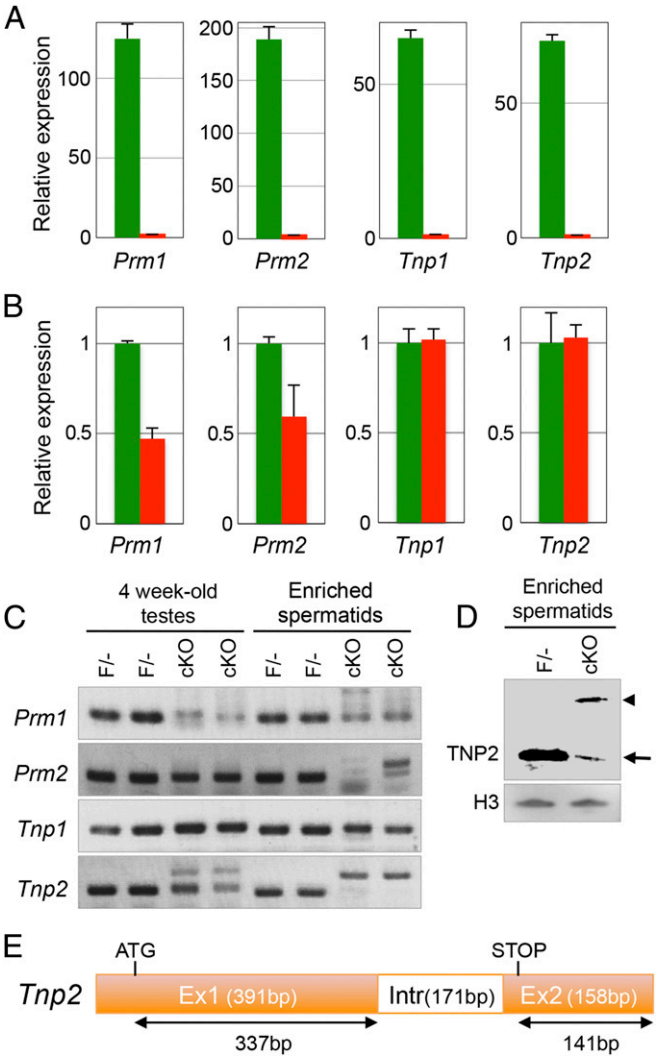

Fig. 4. Splicing defects observed in the absence of MRG15. (*A* and *B*) Quantitative expressions of *Prm1*, *Prm2*, *Tnp1*, and *Tnp2* were examined by quantitative RT-PCR in (*A*) testes and (*B*) spermatid fractions of 22-d-old WT (green) and MRG15 cKO (red) mice. *Hprt* was used as an internal control. (*C*) Validation of the size of the PCR products of *Prm1*, *Prm2*, *Tnp1*, and *Tnp2* in 4-wk-old testes and spermatid fractions of F/– and cKO males by electrophoresis. (*D*) Detection of TNP2 protein in F/– and cKO spermatids. Whole-protein extracts of crude spermatid fractions of F/– and cKO were separated by electrophoresis and probed with anti-TNP2 antibody. Arrow and arrowhead indicate a predicted size of TNP2 and a larger size of intron retained TNP2, respectively. Histone H3 was performed as control. (*E*) Structure of *Tnp2* gene. *Tnp2* mRNA consists of two exons (391 and 158 bp) and one intron (171 bp). The ORF of *Tnp2* is 354 bp. When the intron is retained in the *Tnp2* mRNA, the predicted length is 525 bp.

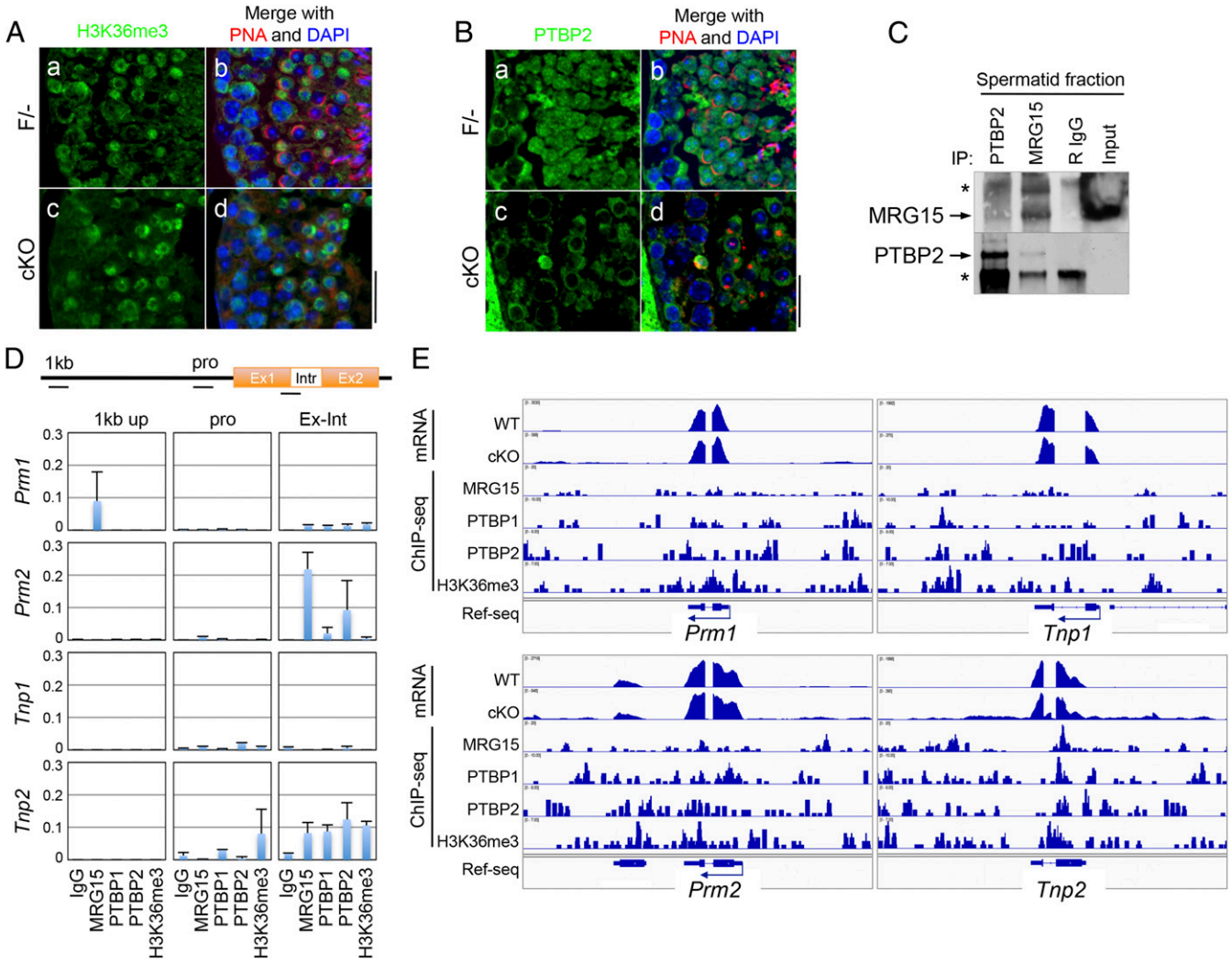

Fig. 5. MRG15 and PTBP2 cooperatively regulate splicing of *Tnp2* gene. (*A*) Accumulation of H3K36me3 in the testes. (*a* and *c*) H3K36me3 (green) and (*b* and *d*) peanut agglutinin (PNA; red) were visualized in the (*a* and *b*) F/– and (*c* and *d*) cKO testes. (*B*) Immunolocalization of PTBP2. (*a* and *c*) PTBP2 (green) and (*b* and *d*) PNA (red) were stained in the (*a* and *b*) F/– and (*c* and *d*) cKO testes. (Scale bar: 50 μm.) (*C*) Coimmunoprecipitation of MRG15 and PTBP2 in WT spermatid fraction. Arrows indicate the bands of each protein. IP, immunoprecipitation; R, rabbit; *, IgG. (*D*) ChIP analyses of the protamine and transition protein genes. Quantitative PCR using primers located on 1-kb upstream, promoter, and exon–intron junction of *Prm1*, *Prm2*, *Tnp1*, and *Tnp2* (each location is shown in *Upper*) was performed in ChIPs with indicated antibodies. Results are shown as relative amplification against input genome. (*E*) Colocalization of retained intron and MRG15 complexes. Genome browser views show the alignment of the read sequences of mRNA and ChIP with MRG15, PTBP1, PTBP2, and H3K36me3 on the mouse genomic regions of *Prm1*, *Prm2*, *Tnp1*, and *Tnp2* of WT spermatids. Ref-seq, reference sequence.

levels in the nucleus of both control and *Mrg15* null round spermatids (Fig. 5*A*), suggesting that H3K36 methylation is not affected by lack of MRG15. MRG15 interacts with PTBP2 in the WT spermatid fractions, and PTBP2 localizes to round spermatids similar to MRG15 and methylated H3K36 (Figs. 5 *A*–*C*). In the absence of MRG15, PTBP2 is excluded from the nuclei of round spermatids, suggesting that recruitment of PTBP2 to the splicing machinery is defective in *Mrg15* null round spermatids (Fig. 5*B*). To further verify the recruitment of PTBP2 to splicing elements by MRG15, localization of MRG15 and PTBP proteins as well as H3K36me3 was analyzed by ChIP. We discovered specific colocalization of MRG15 and PTBP proteins between exons and introns of the *Tnp2* gene but did not discover specific colocalization on either the 1-kb upstream region or the promoter region of the *Tnp2* gene or the *Prm1*, *Prm2*, and *Tnp1* genes (Fig. 5*D*).

To investigate a more widespread link between splicing defects and the lack of MRG15 and MRG15-containing protein complexes, we performed whole-mRNA sequencing and ChIP sequencing (ChIP-seq) against H3K36me3, MRG15, PTBP1, and PTBP2 using enriched spermatids collected from 22- to 25-d-old testes. We found that specific mRNA sequences disappeared from 66 germ cell-expressed genes in the absence of MRG15 and that specific intronic sequences were retained in mRNAs of 4 genes in the MRG15 cKO testes (Tables 1 and 2). In the *Mrg15* null spermatids, colocalization of MRG15 complexes and H3K36me3 near splicing-defective regions was observed in 61 genes that had skipped sequences and all 4 genes that had retained sequences (Tables 1 and 2). Strong colocalization of MRG15, PTBP proteins, and H3K36me3 at the junction between exon and intron of the *Tnp2* gene was confirmed by the ChIP-seq experiments (Fig. 5*E*). Although weak colocalization of the MRG15 complex and H3K36me3 was detected at the junction between exon and intron of *Prm2*, there was only a slight intron retention of the *Prm2* transcript detected in deep sequencing results (Fig. 5*E*). Because the intron of *Tnp2* was retained in its precursor mRNA, other genes, in which an intron sequence remained in their mRNAs in the absence of MRG15, were

Table 1. Genes that have skipped sequences in the absence of MRG15

Gene	Chromosome	Start	Stop	Gene ontology term (biological process)	Gene ontology term (cellular)	Ref.
Ankrd44	Chr1	54,784,415	54,786,577	—	—	
Ccdc93	Chr1	123,383,243	123,387,698	Golgi to plasma membrane transport	Endosome	
Mtap2	Chr1	66,448,096	66,466,708	Microtubule bundle formation	Cytoskeleton	29
Plekha6	Chr1	135,142,720	135,155,585	—	—	
Ptpn4	Chr1	121,680,167	121,698,899	Protein dephosphorylation	Cytoskeleton	
Spata17	Chr1	188,964,376	188,998,253	—	Cytoplasm	35
Ccdc34	Chr2	109,872,597	109,880,730	—	—	
Frmd5	Chr2	121,417,499	121,632,465	—	Cytoskeleton	
Pfkfb3	Chr2	11,401,999	11,403,497	Fructose 2,6-bisphosphate metabolism	Nucleoplasm	46
Zhx3	Chr2	160,658,155	160,698,526	Transcription, DNA templated	Nucleus	
Nbea	Chr3	55,514,662	55,521,698	Protein targeting	Trans-Golgi network	
Pdzk1	Chr3	96,634,080	96,654,150	Calnitine transport	Plasma membrane	
Postn	Chr3	54,181,529	54,187,309	Cell adhesion	Extracellular region	
Sgms2	Chr3	131,045,379	131,047,507	Lipid metabolic process	Golgi apparatus	
Aof2	Chr4	136,110,316	136,111,087	Transcription, DNA templated	Nuclear chromatin	
Eif4g3	Chr4	137,702,289	137,707,496	Translation	—	30
Map3k7	Chr4	32,097,397	32,102,913	MAPK cascade	Plasma membrane	
Pef1	Chr4	129,798,686	129,802,306	Proteolysis	Cytoplasm	
Slc9a1	Chr4	132,972,414	132,973,814	Ion transport	Plasma membrane	
Ssbp3	Chr4	106,703,697	106,709,540	Transcription, DNA templated	Nucleus	
Tssk3	Chr4	129,166,977	129,167,705	Spermatogenesis	Intracellular	
1700023E05Rik	Chr5	77,445,664	77,471,120	—	—	
*4931409K22Rik**	Chr5	24,056,624	24,057,778	—	—	
Prom1	Chr5	44,454,424	44,485,633	Retina-layer formation	Extracellular space	
Cpa5	Chr6	30,561,444	30,562,506	Proteolysis	Extracellular region	
Vgll4	Chr6	114,814,098	114,840,634	Transcription, DNA templated	Nucleus	
Vhlh	Chr6	113,574,373	113,578,085	Transcription, DNA templated	Nucleus	
Eftud1	Chr7	89,846,528	89,899,301	Translation	Intracellular	
*Igf2**	Chr7	149,841,722	149,844,268	Protein phosphorylation	Extracellular region	
Vasp	Chr7	19,843,269	19,844,151	Actin cytoskeleton organization	Cytoskeleton	
Dynlrb2	Chr8	119,038,866	119,039,579	Microtubule-based movement	Cytoskeleton	
Psd3	Chr8	70,314,841	70,341,846	ARF protein signal transduction	Plasma membrane	
Stox2	Chr8	48,288,628	48,437,384	—	—	
Abhd14b	Chr9	106,352,563	106,353,723	Transcription, DNA templated	Nucleus	
*Ccdc33**	Chr9	57,878,228	57,879,421	Spermatogenesis	Peroxisome	
Dixdc1	Chr9	50,519,078	50,535,890	Wnt signaling pathway	Cytoplasm	
Ncam1	Chr9	49,365,344	49,372,973	Cell adhesion	Plasma membrane	
Nptn	Chr9	58,491,610	58,498,303	Cell adhesion	Plasma membrane	
Osbpl10	Chr9	115,085,201	115,116,631	Lipid metabolic process	Cytoskeleton	
Pkm2	Chr9	59,519,881	59,523,374	Glycolytic process	Mitochondrion	
Usp2	Chr9	43,875,304	43,883,448	Protein deubiquitination	Nucleus	31
Hbs1l	Chr10	21,056,882	21,061,519	Translation	Intracellular	
Mtap7	Chr10	19,868,887	19,950,589	Microtubule cytoskeleton organization	Cytoskeleton	32
4933404M19Rik	Chr11	78,017,700	78,018,341	—	—	
Ace	Chr11	105,832,798	105,833,330	Proteolysis	Extracellular region	33
Akap1	Chr11	88,707,180	88,725,710	Regulation of PKA signaling	Mitochondrion	
Ccdc46	Chr11	108,392,780	108,431,601	Receptor localization to synapse	Cytoskeleton	
Tex14	Chr11	87,356,880	87,362,933	Mitotic nuclear division	Kinetochore	34
4930579E17Rik	Chr12	37,274,548	37,414,835	Axon guidance	—	
*Ankrd9**	Chr12	112,215,759	112,216,157	Hydrolase activity	—	
Spata7	Chr12	99,870,248	99,872,433	Response to stimulus	Cytoskeleton	
2010111I01Rik	Chr13	63,383,567	63,398,165	Proteolysis	Cytoplasm	
Bmp6	Chr13	38,438,457	38,561,482	BMP signaling pathway	Extracellular region	
Cdc14b	Chr13	64,297,984	64,306,578	DNA repair	Nucleus	38
4933401F05Rik	Chr14	64,700,689	64,704,147	Proteolysis	Membrane	
Diap3	Chr14	87,172,510	87,210,142	Actin cytoskeleton organization	Nucleus	
Apol7b	Chr15	77,258,240	77,277,809	—	—	
Dab2	Chr15	6,249,900	6,366,805	Endocytosis	Plasma membrane	
Gm628	Chr15	73,623,216	73,629,309	—	—	
Lpp	Chr16	24,681,958	24,761,678	Cell adhesion	Cytoplasm	
AW554918	Chr18	25,362,478	25,448,439	—	—	
Sncaip	Chr18	53,067,129	53,074,960	Cell death	Cytoplasm	
Tcf4	Chr18	69,802,670	69,810,875	Transcription, DNA templated	Nucleus	
6030443O07Rik	Chr19	45,046,176	45,047,623	DNA repair	Nucleus	
Sorbs1	Chr19	40,374,012	40,386,158	Actin filament organization	Cytoskeleton	
*Rpgr**	ChrX	9,743,403	9,755,396	Cilium assembly	Cytoskeleton	36

*These genes have skipped sequences but do not show colocalization of H3K36me3 and MRG15 complexes.

Table 2. Genes with retained sequences in *Mrg15* cKO but not in WT spermatids

Gene	Chromosome	Start	Stop	Intron no.	Full name-location
Mfap5	Chr6	122,471,947	122,474,504	6	Mfap5_chr6_122471947_122474504_6
Nmnat3	Chr9	98,304,033	98,310,495	4	Nmnat3_chr9_98304033_98310495_4
Tpm1	Chr9	66,895,719	66,896,825	1	Tpm1_chr9_66895719_66896825_1
Tnp2	Chr16	10,788,187	10,788,357	1	Tnp2_chr16_10788187_10788357_1

further investigated. Among four genes that had retained sequences, only *Tnp2* retained the whole intron sequence, whereas *Mfap5* and *Nmnat3* retained a part of the intronic sequences, and *Tpm1* retained an exon that was not expressed in MRG15-positive spermatids. We confirmed splicing defects of three genes in the absence of MRG15 and also, weak colocalization of MRG15, PTBPs, and H3K36me3 around each defective locus using mRNA sequencing and ChIP-seq (*SI Appendix*, Fig. S6). The results at least indicate that MRG15 recognizes H3K36me3 and recruits PTBP2 to the splicing machinery of the *Tnp2* gene, and this protein complex regulates pre-mRNA splicing of *Tnp2* cooperatively (Fig. 6).

In addition, at least *Mtap2*, *Eif4g3*, *Usp2*, *Mtap7*, *Ace*, and *Tex14* are known to play a role in male fertility (29–34), and overexpression of *Spata17* and *Rpgr* leads to male infertility (35, 36). Therefore, the infertility in the *Mrg15* cKO mice could be secondary to alterations in the levels of these proteins. For example, our group has described the essential roles of TEX14 in male fertility and formation of intercellular bridges (34). The lack of TEX14 leads to the loss of intercellular bridges and the failure of proliferation and differentiation of spermatogonia (34, 37). Although the roles of TEX14 and intercellular bridges during postmeiotic process still remain to be elucidated, abnormal TEX14 might be a cause of the defects in spermatogenesis in the absence of *Mrg15*. Furthermore, *Mtap2*, *Spata17*, *Frmd5*, *Vasp*, *Dynlrb2*, *Osbpl10*, *Mtap7*, *Ccdc46*, *Spata7*, *Cdc14b*, *Sorbs1*, and *Rpgr* could be important for postmeiotic spermatogenic progression and might also be involved in the defects in the *Mrg15* null germ cells (Table 1) (38); these proteins are associated with microtubules and cytoskeleton, and suppression of their levels could be involved in the formation of multinuclear round spermatids and the failure to form mature sperm.

Discussion

One of the biological events in which MRG15 is involved is homology-directed DNA repair after DNA damage (21). Many proteins that control homology-directed DNA repair, such as RAD51, BRCA1, BRCA2, and PALB2, are also involved in the regulation of meiotic homologous recombination (39–42). When MRG15 is down-regulated in somatic cells, localization of RAD51, BRCA2, and PALB2 to DNA damage sites is suppressed (21). However, the formation of RAD51 foci was not affected by the deletion of MRG15. Although localization of PALB2 to DNA damage sites can be regulated by BRCA1 independently with MRG15 and depletion of PALB2 leads to loss of RAD51 focus formation in the DNA damage sites of somatic cells, inhibition of the interaction between PALB2 and BRCA1 does not affect formation of RAD51 foci in meiotic double-strand breaks, even if it results in male sterility, likely secondary to defect in sex chromosome synapsis (42). Because there were no significant defects in meiosis *Mrg15* null testes, MRG15 is apparently not required for meiotic homologous recombination.

Herein, we found splicing failures in multiple genes in the absence of MRG15 and showed that histone modification regulates splicing via chromatin binding proteins, such as MRG15 (7) (Fig. 6). These splicing forms might produce different products and have different functions from the typical annotated sequences. The results suggest that absence of a spliced form of a gene could be important for progression of spermatogenesis. When an abnormal splicing form is expressed in WT spermatids, the gene product could have different functions compared with the original product. In contrast, the gene product could lose its own function or exert an antagonistic effect on the original product when it is expressed in the *Mrg15* null spermatids. In this study, we focused on the abnormally spliced mRNA, in which intronic sequences remained in the absence of MRG15. Among four genes with retained sequences, strong interaction between MRG15 complexes and abnormal splicing was found in the *Tnp2* gene, whereas weak interaction was found in the other three genes: *Mtap5*, *Nmnat3*, and *Tpm1*. Of note, the retained sequence of *Tpm1* in the absence of MRG15 was derived from an exon but not derived from an intron, indicating that MRG15 complexes could regulate alternatively splicing of *Tpm1*. In addition, skipped exon 3 of *Tpm1* is a known target of PTBP (43). Interestingly, there was slight and weak colocalization of MRG15–PTBPs complexes around introns of *Prm1* and *Prm2*, respectively, despite that H3K36me3 was strongly accumulated at the junction between exon and intron of *Prm1* and *Prm2*. Some other proteins or modifications might participate in the regulation of splicing events of *Tpm1*, *Prm1*, and *Prm2* mRNAs. Because MRG15 can interact with HAT, HDAC complexes, and other histone modifications, such as methylated H4K20, localization of MRG15 on the genome may be regulated by not only H3K36me3 but also, other histone modifications and/or protein complexes (13–21, 26). PTBPs are known to antagonize exon definition; therefore, those retained sequences could be recognized as an exon on the absence of MRG15 (44). Although detailed molecular mechanisms underlying epigenetic regulation of specific sequence retention still remain to be elucidated, amounts of MRG15–PTBPs complexes localized in the regulatory region seem to be correlated with ratios of splicing defects in the lack of MRG15 (Figs. 4*C* and 5*E*). However, many abnormally spliced mRNAs, in which exon sequences were skipped by the lack of MRG15, were identified. MRG15–PTBPs complexes could repress splicing of those skipped sequences in the absence of MRG15. Because *Tnp2* null mice are not sterile, defects in other

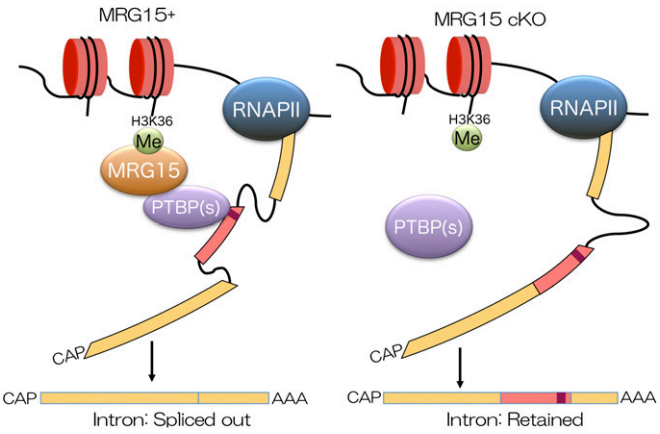

Fig. 6. Proposed model for how MRG15 regulates pre-mRNA splicing of germ cell genes, such as *Tnp2*. AAA, poly A tail of mRNA; CAP, 5′ cap structure of mRNA; Me, methylation; RNAPII, RNA polymerase II.

genes must be involved in the phenotype of the *Mrg15* cKO mice (45). The most apparent defect in *Mrg15* null spermatogenesis was spermatogenic arrest at the round spermatid stage. The epididymides of the *Mrg15* cKO mice were filled with round spermatids, suggesting that the absence of MRG15 might induce splicing defects in the genes, which were essential for round spermatids to proceed to the elongation step. Moreover, multinuclear round spermatids were frequently detected in testes lacking MRG15, indicating that some genes, which were essential for cell division, are altered by the lack of MRG15. Among 61 genes with MRG15-regulated intron skipped sequences, 9 genes are categorized as cytoskeleton-associated genes, and 9 genes are categorized as microtubule, actin, or cytoskeletal protein binding genes (Table 1). Particularly, *Mtap7* is localized in the spermatid manchette, and *Mtap7* mutant mice are sterile because of deformation of spermatid nuclei. Another cytoskeletal-associated gene, *Mtap2*, is required for spermatocytes to exit meiotic prophase I via the G2/MI transition. Although the role of MTAP2 in round spermatids is not known, abnormal MTAP2 could be a cause of the formation of multinuclear round spermatids. CDC14B, which is a dual-specificity phosphatase, could also be involved in the formation of multinuclear round spermatids, because it can bind, bundle, and stabilize microtubules independent of its phosphatase activity (38). However, PFKFB3 could be involved in formation of mature sperm; PFKFB3 is present only in immature sperm and replaced with PFKFB4 during maturation of sperm (46). Thus, splicing defects of multiple genes regulated by MRG15–PTBPs complexes could cause the defects in spermatogenesis in the absence of *Mrg15*. Additional characterization as well as biological analyses of each abnormal splicing form and ChIP-seq using pure spermatids may uncover additional spermatogenic phenotypes in the *Mrg15* null testes.

Germline-specific deletion of *Ptbp2* results in male sterility secondary to defects in alternative splicing (47). In the *Ptbp2* null mice, spermatogenesis also arrests at the round spermatid stage, and there are multinucleated cells as observed in the *Mrg15* null germ cells. These results suggest that MRG15 and PTBP2 share target genes and regulate pre-mRNA splicing cooperatively. However, splicing defects that were found in the absence of PTBP2 were not altered in the *Mrg15* null spermatids, suggesting that MRG15 and PTBP2 share some but not all splicing events (*SI Appendix*, Fig. S6) (47).

A large part of splicing forms could be regulated by other histone modifications and/or chromatin binding proteins but could not be regulated by H3K36me3 and MRG15. In fact, there are several complexes that include chromatin binding proteins (which recognize other histone modifications) and a splicing factor, such as H3K9me3/HP1a/hnRNPs, H3K4me3/CHD1/U2 snRNP, or acetylated H3/GCN5/U2 snRNP (5, 48–51). Splicing regulation via an MRG15–PTBP2 complex may also be physiologically relevant to the brain, because PTBP2 expression is restricted to testis and brain, and MRG15 is ubiquitously expressed (52–54). Moreover, regulation of splicing might be detectable in the hematopoietic lineage, because PTBP3 expression is restricted in hematopoietic cells (55). Thus, splicing regulation may be involved in other tissues, and tissue specificity might be regulated by not only the combination of chromatin binding proteins and splicing regulators present but also, regulation of histone modification. Alternative splicing forms and splicing regulation generate protein diversity; therefore, defects in this system may trigger disease.

Materials and Methods

Generation of Germ Cell-Specific *Mrg15* Null Mice and Fertility Analysis. Details regarding the targeting construct and generation of conditional null allele of MRG15 are in *SI Appendix, SI Materials and Methods*. A germline-specific deletion of *Mrg15* was produced by mating with *Stra8-Cre* mice provided by Robert E. Braun, Jackson Laboratory, Bar Harbor, ME (23). For fertility analysis, 6-wk-old control ($Mrg15^{Fl/-}$:*Stra8-Cre*–) and *Mrg15* cKO ($Mrg15^{Fl/-}$:*Stra8*-Cre+) male littermates were individually bred to WT females. The numbers of litters and pups born per litter were monitored over a 6-mo period. All mouse experiments were performed on a C57BL/6J:129S5 hybrid background in accordance with protocols approved by the Institutional Animal Care and Use Committee of Baylor College of Medicine and the Experimental Animal Care Committee of Kyushu University.

Northern Blot Analysis and Semiquantitative and Quantitative RT-PCR. Total RNA from mouse adult tissue samples and developing testes samples and cultured and isolated cell samples were extracted and subjected to Northern blot, semiquantitative RT-PCR, and quantitative PCR. Detailed methods and the primer sequences used in the experiments can be found in *SI Appendix, SI Materials and Methods* and Table S1, respectively.

Histology, Immunofluorescence, and TUNEL Staining. For testis histology, 5-μm sections were stained with periodic acid-Schiff reagent and counterstained with hematoxylin. For immunofluorescence of tissue sections, paraformaldehyde-fixed sections were retrieved by microwave and then, incubated with primary antibodies overnight at 4 °C followed by Alexa 488- and Alexa 594-conjugated secondary antibodies (Invitrogen) for 1 h at room temperature. Fluorescent sections were mounted with VECTASHIELD containing DAPI (VECTOR Laboratories). To detect apoptotic cells, DNA fragmentation was analyzed by the ApopTag Plus Fluorescein In Situ Apoptosis Detection Kit (Millipore) according to the manufacturer's instruction. Details regarding antibodies are included in *SI Appendix, SI Materials and Methods*.

Chromosome Analysis. Chromosome spread analysis was performed as previously described (56). Antibody information is included in *SI Appendix, SI Materials and Methods*.

ChIP. Approximately 10 million spermatids were cross-linked and sonicated until DNA was fragmented to an average length 200–500 bp. Control immunoprecipitation was performed with normal rabbit IgG. Immunoprecipitated DNA and input DNA were analyzed by PCR using the primers listed in *SI Appendix*, Table S1 or sequenced by Illumina HiSeq1500. Details regarding ChIP and antibodies used can be found in *SI Appendix, SI Materials and Methods*.

RNA Deep Sequencing and ChIP-Seq Analyses. Details regarding RNA deep sequencing, ChIP sequencing, and their analyses are in *SI Appendix, SI Materials and Methods*. RNA sequencing and ChIP-seq data have been deposited in the DDBJ (DNA Data Bank of Japan) Sequence Read Archive under accession numbers DRA004783 and DRA004778, respectively.

ACKNOWLEDGMENTS. We thank Dr. Olivia M. Pereira-Smith for her support and suggestions and Drs. Julio M. Castaneda and John W. Nelson for critical review of the manuscript. We also thank Dr. Robert E. Braun for the gift of the *Stra8-Cre* mice and Megumi Furukawa and Tomona Hayashi for their technical assistance. We thank the Genomic and RNA Profiling Core, Baylor College of Medicine for RNA deep sequencing; and the Research Institute for Information Technology, Kyushu University for ChIP-seq. This work was supported, in part, by the Japan Society for the Promotion of Sciences Grant-in-Aid for Young Scientists Grant 26712026 (to N.I.), Grant 15K21217 (to T.I.), Grant-in-Aid for Scientific Research (KAKENHI) Grant 26114506 (to T.I.), the Takeda Science Foundation (N.I.), Interdisciplinary Programs in Education and Projects in Research Development in Kyushu University (N.I.), and Eunice Kennedy Shriver National Institute of Child Health and Human Development/NIH Cooperative Agreement U01-HD076508 (to M.M.M.) as part of the Cooperative Program in Male Contraception.

1. Oatley JM, Brinster RL (2008) Regulation of spermatogonial stem cell self-renewal in mammals. *Annu Rev Cell Dev Biol* 24:263–286.
2. Kota SK, Feil R (2010) Epigenetic transitions in germ cell development and meiosis. *Dev Cell* 19(5):675–686.
3. Rathke C, Baarends WM, Awe S, Renkawitz-Pohl R (2014) Chromatin dynamics during spermiogenesis. *Biochim Biophys Acta* 1839(3):155–168.
4. Payne C, Braun RE (2006) Histone lysine trimethylation exhibits a distinct perinuclear distribution in Plzf-expressing spermatogonia. *Dev Biol* 293(2):461–472.
5. Luco RF, Allo M, Schor IE, Kornblihtt AR, Misteli T (2011) Epigenetics in alternative pre-mRNA splicing. *Cell* 144(1):16–26.
6. Kalsotra A, Cooper TA (2011) Functional consequences of developmentally regulated alternative splicing. *Nat Rev Genet* 12(10):715–729.
7. Luco RF, et al. (2010) Regulation of alternative splicing by histone modifications. *Science* 327(5968):996–1000.
8. Andersson R, Enroth S, Rada-Iglesias A, Wadelius C, Komorowski J (2009) Nucleosomes are well positioned in exons and carry characteristic histone modifications. *Genome Res* 19(10):1732–1741.

9. Kolasinska-Zwierz P, et al. (2009) Differential chromatin marking of introns and expressed exons by H3K36me3. *Nat Genet* 41(3):376–381.
10. Schwartz S, Meshorer E, Ast G (2009) Chromatin organization marks exon-intron structure. *Nat Struct Mol Biol* 16(9):990–995.
11. Spies N, Nielsen CB, Padgett RA, Burge CB (2009) Biased chromatin signatures around polyadenylation sites and exons. *Mol Cell* 36(2):245–254.
12. Tilgner H, et al. (2009) Nucleosome positioning as a determinant of exon recognition. *Nat Struct Mol Biol* 16(9):996–1001.
13. Chen M, Tominaga K, Pereira-Smith OM (2010) Emerging role of the MORF/MRG gene family in various biological processes, including aging. *Ann N Y Acad Sci* 1197: 134–141.
14. Yochum GS, Ayer DE (2002) Role for the mortality factors MORF4, MRGX, and MRG15 in transcriptional repression via associations with Pf1, mSin3A, and Transducin-Like Enhancer of Split. *Mol Cell Biol* 22(22):7868–7876.
15. Cai Y, et al. (2003) Identification of new subunits of the multiprotein mammalian TRRAP/TIP60-containing histone acetyltransferase complex. *J Biol Chem* 278(44): 42733–42736.
16. Doyon Y, Selleck W, Lane WS, Tan S, Côté J (2004) Structural and functional conservation of the NuA4 histone acetyltransferase complex from yeast to humans. *Mol Cell Biol* 24(5):1884–1896.
17. Hayakawa T, et al. (2007) RBP2 is an MRG15 complex component and down-regulates intragenic histone H3 lysine 4 methylation. *Genes Cells* 12(6):811–826.
18. Sardiu ME, et al. (2008) Probabilistic assembly of human protein interaction networks from label-free quantitative proteomics. *Proc Natl Acad Sci USA* 105(5):1454–1459.
19. Kusch T, et al. (2004) Acetylation by Tip60 is required for selective histone variant exchange at DNA lesions. *Science* 306(5704):2084–2087.
20. Sy SMH, Huen MSY, Chen J (2009) MRG15 is a novel PALB2-interacting factor involved in homologous recombination. *J Biol Chem* 284(32):21127–21131.
21. Hayakawa T, et al. (2010) MRG15 binds directly to PALB2 and stimulates homology-directed repair of chromosomal breaks. *J Cell Sci* 123(Pt 7):1124–1130.
22. Tominaga K, et al. (2005) MRG15 regulates embryonic development and cell proliferation. *Mol Cell Biol* 25(8):2924–2937.
23. Sadate-Ngatchou PI, Payne CJ, Dearth AT, Braun RE (2008) Cre recombinase activity specific to postnatal, premeiotic male germ cells in transgenic mice. *Genesis* 46(12): 738–742.
24. Garcia SN, Kirtane BM, Podlutsky AJ, Pereira-Smith OM, Tominaga K (2007) Mrg15 null and heterozygous mouse embryonic fibroblasts exhibit DNA-repair defects post exposure to gamma ionizing radiation. *FEBS Lett* 581(27):5275–5281.
25. Sun B, et al. (2008) Molecular basis of the interaction of Saccharomyces cerevisiae Eaf3 chromo domain with methylated H3K36. *J Biol Chem* 283(52):36504–36512.
26. Moore SA, Ferhatoglu Y, Jia Y, Al-Jiab RA, Scott MJ (2010) Structural and biochemical studies on the chromo-barrel domain of male specific lethal 3 (MSL3) reveal a binding preference for mono- or dimethyllysine 20 on histone H4. *J Biol Chem* 285(52): 40879–40890.
27. Meistrich ML, Trostle-Weige PK, Lin R, Bhatnagar YM, Allis CD (1992) Highly acetylated H4 is associated with histone displacement in rat spermatids. *Mol Reprod Dev* 31(3):170–181.
28. Lahn BT, et al. (2002) Previously uncharacterized histone acetyltransferases implicated in mammalian spermatogenesis. *Proc Natl Acad Sci USA* 99(13):8707–8712.
29. Sun F, Handel MA (2011) A mutation in *Mtap2* is associated with arrest of mammalian spermatocytes before the first meiotic division. *Genes (Basel)* 2(1):21–35.
30. Sun F, Palmer K, Handel MA (2010) Mutation of Eif4g3, encoding a eukaryotic translation initiation factor, causes male infertility and meiotic arrest of mouse spermatocytes. *Development* 137(10):1699–1707.
31. Bedard N, et al. (2011) Mice lacking the USP2 deubiquitinating enzyme have severe male subfertility associated with defects in fertilization and sperm motility. *Biol Reprod* 85(3):594–604.
32. Komada M, McLean DJ, Griswold MD, Russell LD, Soriano P (2000) E-MAP-115, encoding a microtubule-associated protein, is a retinoic acid-inducible gene required for spermatogenesis. *Genes Dev* 14(11):1332–1342.
33. Hagaman JR, et al. (1998) Angiotensin-converting enzyme and male fertility. *Proc Natl Acad Sci USA* 95(5):2552–2557.
34. Greenbaum MP, et al. (2006) TEX14 is essential for intercellular bridges and fertility in male mice. *Proc Natl Acad Sci USA* 103(13):4982–4987.
35. Nie DS, Liu Y, Juan H, Yang X (2013) Overexpression of human SPATA17 protein induces germ cell apoptosis in transgenic male mice. *Mol Biol Rep* 40(2):1905–1910.
36. Brunner S, et al. (2008) Overexpression of RPGR leads to male infertility in mice due to defects in flagellar assembly. *Biol Reprod* 79(4):608–617.
37. Iwamori N, Iwamori T, Matzuk MM (2012) Characterization of spermatogonial stem cells lacking intercellular bridges and genetic replacement of a mutation in spermatogonial stem cells. *PLoS One* 7(6):e38914.
38. Cho HP, et al. (2005) The dual-specificity phosphatase CDC14B bundles and stabilizes microtubules. *Mol Cell Biol* 25(11):4541–4551.
39. Plug AW, Xu J, Reddy G, Golub EI, Ashley T (1996) Presynaptic association of Rad51 protein with selected sites in meiotic chromatin. *Proc Natl Acad Sci USA* 93(12): 5920–5924.
40. Scully R, et al. (1997) Association of BRCA1 with Rad51 in mitotic and meiotic cells. *Cell* 88(2):265–275.
41. Sharan SK, et al. (2004) BRCA2 deficiency in mice leads to meiotic impairment and infertility. *Development* 131(1):131–142.
42. Simhadri S, et al. (2014) Male fertility defect associated with disrupted BRCA1-PALB2 interaction in mice. *J Biol Chem* 289(35):24617–24629.
43. Gooding C, et al. (2013) MBNL1 and PTB cooperate to repress splicing of Tpm1 exon 3. *Nucleic Acids Res* 41(9):4765–4782.
44. Sharma S, Kohlstaedt LA, Damianov A, Rio DC, Black DL (2008) Polypyrimidine tract binding protein controls the transition from exon definition to an intron defined spliceosome. *Nat Struct Mol Biol* 15(2):183–191.
45. Zhao M, et al. (2001) Targeted disruption of the transition protein 2 gene affects sperm chromatin structure and reduces fertility in mice. *Mol Cell Biol* 21(21): 7243–7255.
46. Gómez M, et al. (2009) Switches in 6-phosphofructo-2-kinase isoenzyme expression during rat sperm maturation. *Biochem Biophys Res Commun* 387(2):330–335.
47. Zagore LL, et al. (2015) RNA binding protein Ptbp2 is essential for male germ cell development. *Mol Cell Biol* 35(23):4030–4042.
48. Sims RJ, 3rd, et al. (2007) Recognition of trimethylated histone H3 lysine 4 facilitates the recruitment of transcription postinitiation factors and pre-mRNA splicing. *Mol Cell* 28(4):665–676.
49. Gunderson FQ, Johnson TL (2009) Acetylation by the transcriptional coactivator Gcn5 plays a novel role in co-transcriptional spliceosome assembly. *PLoS Genet* 5(10): e1000682.
50. Piacentini L, et al. (2009) Heterochromatin protein 1 (HP1a) positively regulates euchromatic gene expression through RNA transcript association and interaction with hnRNPs in Drosophila. *PLoS Genet* 5(10):e1000670.
51. Loomis RJ, et al. (2009) Chromatin binding of SRp20 and ASF/SF2 and dissociation from mitotic chromosomes is modulated by histone H3 serine 10 phosphorylation. *Mol Cell* 33(4):450–461.
52. Polydorides AD, Okano HJ, Yang YY, Stefani G, Darnell RB (2000) A brain-enriched polypyrimidine tract-binding protein antagonizes the ability of Nova to regulate neuron-specific alternative splicing. *Proc Natl Acad Sci USA* 97(12):6350–6355.
53. Markovtsov V, et al. (2000) Cooperative assembly of an hnRNP complex induced by a tissue-specific homolog of polypyrimidine tract binding protein. *Mol Cell Biol* 20(20): 7463–7479.
54. Xu M, Hecht NB (2007) Polypyrimidine tract binding protein 2 stabilizes phosphoglycerate kinase 2 mRNA in murine male germ cells by binding to its 3′UTR. *Biol Reprod* 76(6):1025–1033.
55. Yamamoto H, Tsukahara K, Kanaoka Y, Jinno S, Okayama H (1999) Isolation of a mammalian homologue of a fission yeast differentiation regulator. *Mol Cell Biol* 19(5):3829–3841.
56. Iwamori N, Zhao M, Meistrich ML, Matzuk MM (2011) The testis-enriched histone demethylase, KDM4D, regulates methylation of histone H3 lysine 9 during spermatogenesis in the mouse but is dispensable for fertility. *Biol Reprod* 84(6): 1225–1234.